MOLECULAR AND CELLULAR BIOLOGY, Nov. 2008, p. 6954–6966 Vol. 28, No. 22
0270-7306/08/$08.00+0 doi:10.1128/MCB.00925-08

Extracellular Signal-Regulated Kinase 2 (ERK2) Phosphorylation Sites and Docking Domain on the Nuclear Pore Complex Protein Tpr Cooperatively Regulate ERK2-Tpr Interaction[▽]

Tomáš Vomastek,[3]§ Marcin P. Iwanicki,[2]§ W. Richard Burack,[4] Divya Tiwari,[1] Devanand Kumar,[1] J. Thomas Parsons,[2] Michael J. Weber,[2]* and Vinay Kumar Nandicoori[1]*

National Institute of Immunology, Aruna Asaf Ali Marg, New Delhi 110 067, India[1]; Department of Microbiology and Cancer Center, University of Virginia Health Sciences Center, P.O. Box 800734, Charlottesville, Virginia 22908-0734[2]; Cell and Molecular Microbiology Division, Institute of Microbiology, Prague, Czech Republic[3]; and University of Rochester Medical Center, 601 Elmwood Ave., Rochester, New York 14642-8626[4]

Received 10 June 2008/Returned for modification 1 August 2008/Accepted 9 September 2008

Identifying direct substrates of mitogen-activated protein kinases (MAPKs) and understanding how those substrates are selected is central to understanding how these ubiquitously activated enzymes generate diverse biological responses. In previous work, we identified several new candidate substrates for the MAPK ERK2 (*e*xtracellular signal-*r*egulated *k*inase 2), including the nuclear pore complex protein Tpr (*t*ranslocated *p*romoter *r*egion). In this report, we identify sites on Tpr for ERK2 phosphorylation and binding and demonstrate their functional interaction. ERK2 phosphorylation and dimerization are necessary for ERK2-Tpr binding, and this occurs through a DEF (*d*ocking site for *E*RK2, *F*XF) domain on Tpr. Surprisingly, the DEF domain and the phosphorylation sites displayed positive cooperativity to promote ERK2 binding to Tpr, in contrast to substrates where phosphorylation reduces binding. Ectopic expression or depletion of Tpr resulted in decreased movement of activated ERK2 from the cytoplasm to the nucleus, implying a role for Tpr in ERK2 translocation. Collectively, the data provide direct evidence that a component of the nuclear pore complex is a bona fide substrate of ERK2 in vivo and that activated ERK2 stably associates with this substrate after phosphorylation, where it could play a continuing role in nuclear pore function. We propose that Tpr is both a substrate and a scaffold for activated ERKs.

The mitogen-activated protein kinase/extracellular signal-regulated kinase (MAPK/ERK) pathway regulates many cellular processes, including proliferation, differentiation, transcription, and cellular motility (28). MAPKs are activated via a kinase cascade that results in their dual phosphorylation on tyrosine and threonine and their consequent activation (6). Although a great deal is known about the biochemical steps involved in the transduction of signals through this pathway, considerably less is known about how these signals are converted into specific biological responses. Understanding this process of signal implementation will require identification of the in vivo substrates of the MAPKs. Although over 150 possible ERK substrates have been reported (49), in very few cases has it been demonstrated that these proteins are in vivo substrates and that MAPK is directly responsible for the phosphorylation.

In the inactive state the ERKs are anchored in the cytoplasm by their association with the MAPK/ERK kinases (MEKs) and several other proteins. Upon activation, the ERKs are released from their anchor and migrate to the nucleus, where they phosphorylate several transcription factors (such as Ets factors) and play an important role in transcriptional regulation (5, 7, 12, 18, 22, 45). Nuclear localization of ERKs can be brought about by either passive diffusion of monomers or active transport (1). Interaction with nucleoporins such as Nup153 and Nup214 has also been suggested to play a role in localization of ERK2 to the nucleus (26, 46), but virtually nothing is known about the ERK partners and substrates that might play a role in this process or in aspects of posttranscriptional gene regulation.

Once at their sites of action, ERKs recognize and phosphorylate serine or threonine residues in the sequence context of S/TP or PXS/TP (17). However, the specificity of the interaction and phosphorylation comes also from docking motifs on the substrates. Two different kinds of domains or motifs have been identified on candidate ERK substrates. The first is a KIM (*k*inase-*i*nteracting *m*otif, also known as a D domain) which consists of a stretch of basic amino acids surrounded by aliphatic hydrophobic residues (leucines, isoleucines, or valines) (3, 38, 42, 50). The second is a DEF domain (*d*ocking site for *E*RK, *F*XF) consisting of two phenylalanine residues separated by one residue, followed by a proline (FXFP), although the proline residue is not essential (11, 15, 21, 43).

To understand the functions of the pathway, identifying and characterizing the direct in vivo targets of ERK phosphorylation and analyzing the molecular basis for substrate specificity

* Corresponding author. Mailing address for Vinay Kumar Nandicoori: National Institute of Immunology, Aruna Asaf Ali Marg, New Delhi 110 067, India. Phone: (91) 11-26703789. Fax: (91) 11-26742125. E-mail: vinaykn@nii.res.in. Mailing address for Michael J. Weber: Department of Microbiology and Cancer Center, University of Virginia Health Sciences Center, P.O. Box 800734, Charlottesville, VA 22908-0734. Phone: (434) 924-5022. Fax: (434) 982-0689. E-mail: mjw@virginia.edu.

§ These authors contributed equally to this work.

▽ Published ahead of print on 15 September 2008.

are of primary importance. In a previous report (10), we identified candidate ERK substrates in cell lysates using a method developed by Shokat and colleagues, in which a structural "pocket" is engineered into protein kinases so that they can utilize ATP orthologs that have bulky substituents (37). In addition to the known ERK2 substrate Rsk2, two novel substrates, E3 ubiquitin ligase EDD (*E*3 identified by *d*ifferential *d*isplay) and nuclear pore complex protein Tpr (*t*ranslocated *p*romoter *r*egion), were found to associate with and be phosphorylated by the ERK2 pocket mutant.

Tpr was originally identified by its fusion (short fragments of Tpr) to various proto-oncogenes such as *met* and *raf* (19, 23, 29). Tpr localizes to the nuclear basket of the nuclear pore complex and is also found in the nucleus in the form of discrete foci (14). The functions of Tpr are poorly understood, but several lines of evidence indicate that it is involved in the process of nuclear export. Tpr has been shown to have a role in the nuclear export of proteins containing a leucine-rich nuclear export signal (14) and in the nuclear export of Huntingtin, a protein with no obvious nuclear export signal (8). Ectopic expression of mammalian Tpr has also been reported to result in accumulation of poly(A)$^+$ RNA in the nucleus (2).

In this report, we characterize Tpr-ERK2 interactions and phosphorylation of Tpr by ERK2 in vitro and in vivo. We identify structural elements in Tpr and ERK2 important for Tpr and ERK association. ERK2 interacts with Tpr through positive cooperative interactions of DEF and the ERK phosphorylation sites. This is in contrast to the other ERK substrates identified with the "pocket mutant" technique, which display decreased binding following phosphorylation. Because phosphorylation of Tpr by activated ERK stabilizes their interaction, we hypothesize that this phosphorylation is not part of a signal amplification cascade but rather positions activated ERK to perform a continuing function in the nuclear pore. We also show that depletion of Tpr results in decreased nuclear accumulation of activated ERK2, suggesting a role for Tpr in modulating ERK2 translocation into the nucleus.

MATERIALS AND METHODS

Reagents, constructs, and mutagenesis. COS-1 cells were from the American Type Culture Collection (ATCC, Manassas, VA) and were maintained in Dulbecco's modified Eagle's medium (Invitrogen, Carlsbad, CA) with 5% fetal bovine serum (Invitrogen). Anti-FLAG-M2 monoclonal antibodies and anti-FLAG-M2 agarose affinity beads were from Sigma (St. Louis, MO). Monoclonal anti-hemagglutinin (HA) antiserum 12CA5 was purchased from Covance, Berkeley, CA. Constructs of Tpr antibodies (raised against amino acid residues 2095 to 2348), full-length Tpr fused to enhanced green fluorescent protein (EGFP-Tpr), and the C-terminal portion of Tpr fused to HA epitope (HA-TprC; amino acids 1626 to 2340) were kindly provided by L. Gerace (The Scripps Research Institute, La Jolla, CA) (2, 14). The FLAG-ERK2 construct has been previously described (40). FLAG-ERK2-T183AY185F (TAYF) and FLAG-ERK2-K52R constructs were generated by PCR mutagenesis. The ERK2-Δ4 mutant was a gift from M. H. Cobb, University of Texas Southwestern Medical Center, Dallas, TX (32). ERK2-Δ4 was subcloned into FLAG-ERK2 to generate FLAG-ERK2-Δ4.

The JNK1 construct was provided by Roger Davis, University of Massachusetts Medical School, Boston, MA (9), and the GST-p38α construct was provided by Dennis J. Templeton, University of Virginia, VA (36). pcDNA3-FLAG-JNK1 and pcDNA3-FLAG-p38α constructs were generated by amplifying JNK1 and p38α coding regions by PCR and subcloning the products into pcDNA3-FLAG vector. FLAG-tagged Tpr C-terminal (FLAG-TprC; amino acids 1626 to 2349) and FLAG-tagged Tpr N-terminal (FLAG-TprN; amino acids 1 to 800) constructs were generated by PCR amplification of the respective regions using EGFP-TprFL (14) as a template. PCR products were digested with NotI and ApaI (introduced through primers) and subcloned into the same sites in pcDNA3-FLAG vector. FLAG-tagged full-length Tpr (TprFL) was generated by ligating the NotI-BmtI fragment from FLAG-TprN and the BmtI-PpuMI fragment from pGFP-Tpr and subcloning into NotI-PpuMI sites of FLAG-TprC vector. FLAG-ERK2-DD→NN, FLAG-ERK2 L232A, and various FLAG-TprC mutants were generated by PCR mutagenesis.

Immunoprecipitation. Dishes (100 mm) of COS-1 cells (2.4×10^6 to 3×10^6 cells) were transfected using Lipofectamine 2000 (Invitrogen) according to the manufacturer's recommendations. Cells were allowed to recover overnight, and transfected cells were then serum starved for 4 to 5 h and stimulated either with epidermal growth factor (EGF) (20 ng/ml) for 10 min or with anisomycin (1 μM) for 30 min. Immunoprecipitation was carried out as described previously (10).

In vitro kinase reactions and phosphoamino acid and phosphopeptide analysis. After transfection and immunoprecipitation as described above, the immunoprecipitated FLAG-TprFL, FLAG-TprC, and mutants of FLAG-TprC or the vector control were mixed with immunoprecipitated ERK2, and kinase reactions were performed in 25 mM HEPES (pH 7.4), 20 mM magnesium acetate, and 1 mM dithiothreitol containing 10 μCi [γ-^{32}P]ATP (Perkin Elmer, Boston, MA), for 10 min at 30°C. Phosphoamino acid and tryptic peptide analysis were performed as described previously (4, 10).

Metabolic labeling and phosphopeptide analysis. Dishes (100 mm) of COS-1 cells were transfected with 10 μg of FLAG-Tpr constructs and were allowed to recover overnight. Cells were washed twice with phosphate-free RPMI medium and starved for 1 h in phosphate-free RPMI medium (Invitrogen). Cultures were metabolically labeled in phosphate-free RPMI medium containing 3 mCi/ml carrier-free $^{32}P_i$ (Perkin Elmer) for 3 h. For EGF-stimulated samples, EGF (20 ng/ml for 10 min) was added to the above medium. Cultures treated with the MEK inhibitor UO126 (Calbiochem, La Jolla, CA) were incubated with 20 μM inhibitor during the 3-h labeling and the EGF stimulation. Immunoprecipitation and tryptic peptide analysis were performed as described previously (10).

Immunoprecipitations, kinase assays, and two-dimensional gel electrophoresis. ^{32}P-labeling of cyclopentyl ADP (cpADP) was carried out as described previously (10). Two 150-mm dishes of COS-1 cells (5×10^6 cells) were cotransfected with 6 μg of HA-ERK2 or HA-ERK2-QG and 12 μg of pcDNA3 or FLAG-TprFL or FLAG-TprFL-FXF→AXA,M4 and were allowed to recover overnight. Transfected cells were then serum starved for 4 to 5 h and stimulated with EGF (20 ng/ml) for 10 min. Immunoprecipitation, kinase assay, and two-dimensional gel electrophoresis were essentially performed as described previously (10).

Ectopic expression, siRNA attenuation of Tpr, and dynamic analysis of ERK in HEK293T cells. A double-stranded small interfering RNA (siRNA) targeting 5′ GCACAACAGGATAAGGTTA 3′ of the *Tpr* gene was purchased from Qiagen Inc. (Valencia, CA). The control siRNA duplex pool (nonspecific control duplex XIII) was purchased from Dharmacon (Lafayette, CO). HEK293T cells were plated in media containing 10% serum on 10 μg/ml fibronectin on 5 μg/ml collagen type IV-coated tissue culture dishes. The following day, cells were transfected using Polyfect reagent (for plasmid constructs) (Qiagen) or calcium phosphate (for siRNA) with 400 ng cyan fluorescent protein (CFP)-MEK1, 400 ng yellow fluorescent protein (YFP)-ERK, and 1 μg of pcDNA3 or 1 μg FLAG-TprFL or with control siRNA or Tpr siRNA. Twenty-four hours posttransfection, cells were serum starved for 3 h and stimulated with EGF (10 ng/ml). The cellular dynamics of YFP-ERK2 and CFP-MEK were captured using a Nikon Eclipse TE2000-E inverted microscope. To quantify YFP-ERK recruitment into the nucleus, the fluorescent intensity of nuclear YFP-ERK was divided by the total intensity (cytoplasmic plus nuclear intensity) of YFP-ERK plus CFP-MEK (YFP/CFP + YFP). Image analysis was performed using Image J software (Wayne Rasband, National Institutes of Health).

Immunofluorescence. Dishes (60 mm) of COS-1 cells (6×10^5 cells) were transfected with 1.5 μg of GFP-Tpr constructs using Lipofectamine 2000. Cells were trypsinized and plated on coverslips in a six-well dish 24 h after transfection and allowed to recover for 48 h. Cells were washed twice with phosphate-buffered saline and fixed with 3% paraformaldehyde for 20 min followed by extraction with cold methanol for 5 min at −20°C. Coverslips were mounted on slides using Vectashield mounting medium (Vector, Burlingame, CA), and cells were examined under a confocal microscope (Zeiss LSM 510 microscope; University of Virginia Advanced Microscopy Facility).

RESULTS

The carboxy terminus of Tpr is sufficient for interaction with activated ERK2. To characterize the ERK2-Tpr interaction, FLAG-ERK2 or the ERK2 "pocket" mutant ERK2-Q103G (ERK2-QG), which can utilize analog ATP as the substrate,

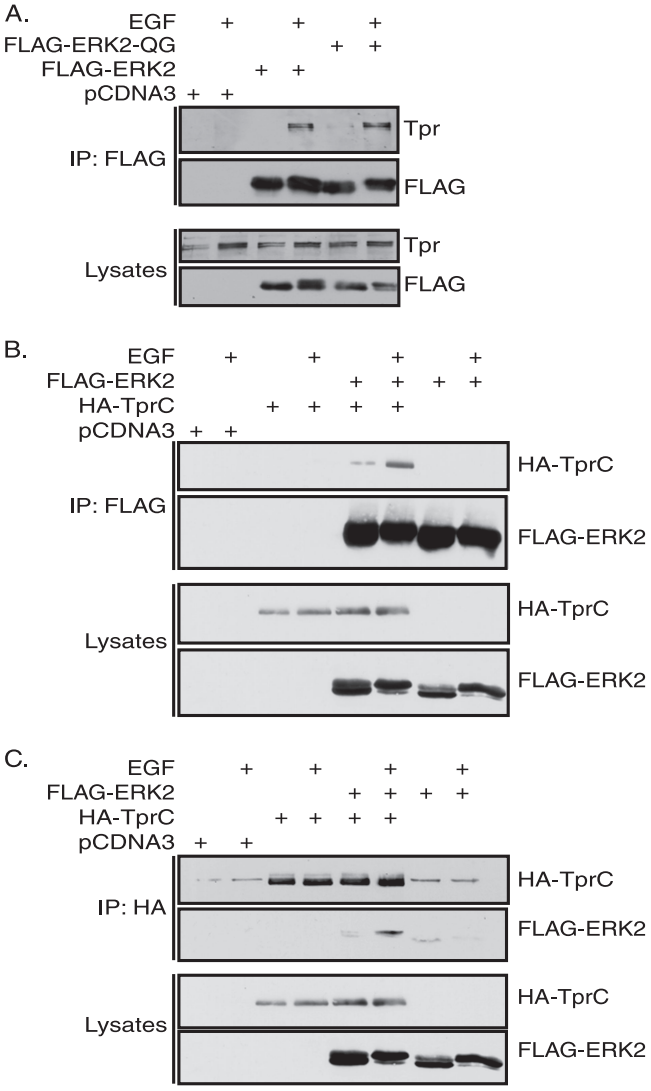

FIG. 1. Carboxy terminus of Tpr is sufficient for association with ERK2 upon EGF stimulation. (A) Cells transfected with pcDNA3, FLAG-ERK2, and FLAG-ERK2-QG were serum starved for 4 to 5 h followed by stimulation with EGF (20 ng/ml) for 10 min. Cells were lysed and proteins immunoprecipitated (IP) with FLAG-M2 agarose beads. Immunoprecipitated proteins were resolved by 10% SDS-PAGE, followed by immunoblotting with anti-FLAG-M2 or anti-Tpr antibodies. (B) Cells transfected with pcDNA3, HA-TprC, FLAG-ERK2, or FLAG-ERK2 and HA-TprC together were serum starved and stimulated with EGF. Proteins were immunoprecipitated and analyzed by immunoblotting as described for panel A and probed with anti-FLAG-M2 and anti-HA antibodies. (C) As in panel B, except that the proteins were immunoprecipitated with anti-HA antibodies coupled to protein A agarose, followed by immunoblotting with anti-FLAG-M2 and anti-HA antibodies.

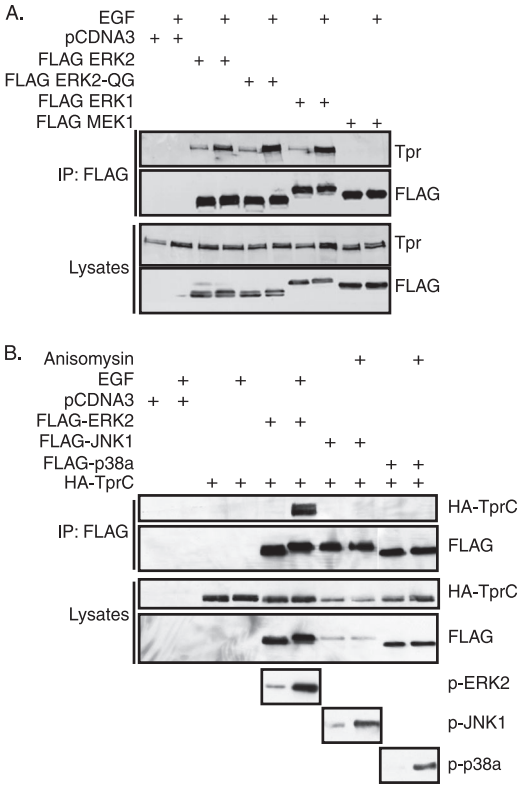

FIG. 2. Tpr does not interact with MEK1, JNK1, or p38α. (A) Cells transfected with pcDNA3, FLAG-ERK2, FLAG-ERK2-QG, FLAG-ERK1, and FLAG-MEK1 were serum starved and stimulated with EGF. Cells were lysed and proteins immunoprecipitated (IP) with FLAG-M2 agarose beads followed by immunoblotting with anti-Tpr and anti-FLAG-M2 antibodies. (B) Cells were transfected with pcDNA3 or HA-TprC, or double transfected with HA-TprC and FLAG-ERK2 or FLAG-JNK1 or FLAG-p38α. The last two were stimulated with anisomycin for 30 min instead of EGF. Cell lysates were probed with anti-FLAG-M2 and anti-HA antibodies. Based on these results, twice the amount of lysate was used for immunoprecipitation from cells cotransfected with FLAG-JNK1 and HA-TprC, compared to amounts for other transfected cells. Proteins were immunoprecipitated with FLAG-M2 agarose beads. One-twentieth of the immunoprecipitated proteins was analyzed by probing with anti-FLAG-M2, anti-phosphor-ERK2 (Sigma), anti-phosphor-JNK1 (Sigma), and anti-phospho-p38α (Sigma). The remaining immunoprecipitated proteins were probed with anti-HA antibodies.

was immunoprecipitated and the immunocomplexes were probed with anti-Tpr antibodies. The association of endogenous Tpr with ERK2 or ERK2-QG in serum-starved cells was weak but increased following EGF stimulation (Fig. 1A). Analysis of the primary sequence of Tpr revealed the presence of a putative KIM (or D domain) and a putative DEF motif in the C-terminal 800-amino-acid region that could be involved in its association with ERK2. Like full-length Tpr (Fig. 1A), HA-TprC (C-terminal fragment) interacted strongly with FLAG-ERK2 when cells were stimulated with EGF (Fig. 1B). In a reverse experiment, HA-TprC was immunoprecipitated and the FLAG-ERK2 interaction with Tpr was examined. A robust association of FLAG-ERK2 with HA-Tpr was evident in EGF-stimulated cells (Fig. 1C). These results indicate that Tpr associates strongly with ERK2 following EGF stimulation, and the C-terminal 800 amino acids of Tpr are sufficient for this interaction.

Tpr does not interact with MEK1, JNK1, or p38α. To test the specificity of the interaction of Tpr with ERK2, we examined possible associations of Tpr with other MAPK pathway proteins as well. Endogenous Tpr associated strongly with ERK2, ERK2-QG, and ERK1, following stimulation with EGF (Fig. 2A). We also detected the association of Tpr with ERK2 and ERK1 in unstimulated reactions, albeit at much lower

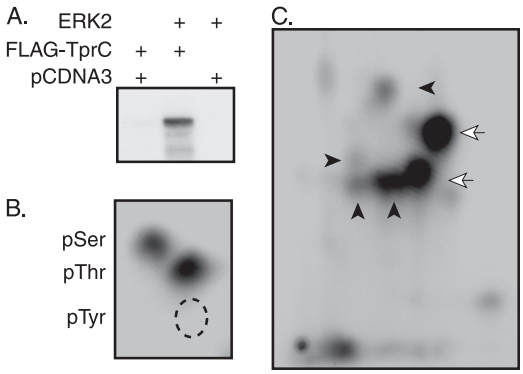

FIG. 3. ERK2 phosphorylates serine and threonine residues of Tpr in vitro. (A) Cells were transfected individually with FLAG-ERK2, FLAG-TprC, and pcDNA3 vectors. Cells were serum starved, and FLAG-ERK2-transfected cells were stimulated with EGF. Proteins were immunoprecipitated from lysed cells with FLAG-M2 agarose beads, and FLAG-ERK2 immunoprecipitate was mixed either with FLAG-TprC immunoprecipitate or with immunoprecipitate from pcDNA3-transfected cells. Kinase reactions were carried out with [γ-^{32}P]ATP at 30°C for 10 min. (B) Phosphoamino acid analysis of in vitro-labeled TprC from time course reactions. p, phosphorylated. (C) In vitro phosphorylated TprC was digested with trypsin, and the resulting phosphopeptides were mapped by two-dimensional TLC (4). Two major spots are indicated by white arrows, and four minor spots are indicated by black arrows.

levels (Fig. 2A). A possible reason for this is the presence of low levels of activated ERKs in these cells even during serum starvation. No interaction between Tpr and MEK1 (Fig. 2A) was detected. These results suggest that the interaction of Tpr with ERK2 and ERK1 is specific and most likely requires activated ERKs. To examine Tpr interactions with JNK1 and p38α, we coexpressed HA-TprC and FLAG-tagged ERK2, JNK1, or p38α. It was evident from the lysate analysis (Fig. 2B) that expression levels of FLAG-JNK1 and HA-TprC in JNK-TprC-cotransfected cells were ~2- to 3-fold lower than the expression levels of ERK2 and p38α and the corresponding HA-TprC levels. To compensate for the lower expression of JNK and TprC, twofold more lysate was used in immunoprecipitations. Results obtained with phospho-antibodies demonstrated efficient activation of MAPKs following stimulation (Fig. 2B). No associations between HA-TprC and MAPKs JNK1 and p38α were observed, irrespective of the activation statuses of these two kinases (Fig. 2B). These data demonstrate that Tpr interacts specifically with the ERKs and not with MEK1, JNK1, and p38α.

ERK2 phosphorylates serine and threonine residues of Tpr in vitro. The primary sequence of Tpr contains 20 ERK2 consensus sequence target sites: one SP and two TP sites within the N-terminal 1,600 amino acids, and 3 SP and 14 TP sites within the C-terminal 800 amino acids. Since the C-terminal 800 amino acids are sufficient for interaction with ERK2, we tested this fragment for possible in vitro phosphorylation. Results demonstrated phosphorylation of FLAG-TprC by ERK2 (Fig. 3A). TprC phosphorylation by ERK2 was evident, and it was more efficient than that of the canonical in vitro substrate myelin basic protein (data not shown). Phosphoamino acid analysis showed phosphorylation of both serine and threonine residues (Fig. 3B), and thus we could not rule out any of the 17 putative target sites. Two-dimensional tryptic phosphopeptide maps of in vitro-phosphorylated Tpr (Fig. 3C) showed that the bulk of the phosphorylation was concentrated in two spots and minor phosphorylation was apparent in four other spots. A similar experiment performed with FLAG-TprN (N-terminal 800 amino acids containing the remaining three target sites) showed that TprN was not phosphorylated by ERK2 in vitro (data not shown). To further confirm that the N-terminal domain of Tpr is not phosphorylated by ERK2, we compared the peptide maps for in vitro-labeled full-length Tpr (TprFL) with that of the C-terminal domain of Tpr (TprC). Two-dimensional tryptic phosphopeptide maps of in vitro-phosphorylated TprFL and TprC showed similar patterns (Fig. 4A), suggesting that TprFL and TprC were phosphorylated on the same sites.

Tpr is phosphorylated by ERK2 at four different sites. We mutagenized all 17 putative target sites individually from serine or threonine to alanine, to determine which sites would alter the two-dimensional tryptic phosphopeptide maps. Thirteen of the seventeen mutants had the same pattern of tryptic phosphopeptides as TprC (data not shown). Four mutants (T2102A, T2123A, S2141A, and T2200A) displayed altered maps (Fig. 4A). Mutation in T2123 resulted in the loss of two spots that were numbered 4 and 4*. The presence of two spots for a monophosphorylated peptide could be due to incomplete digestion by trypsin. Four combination target site mutants were made. These included one with both major sites mutated (Fig. 4B, top panel; TprCM2), a second with the two major sites and one minor site T2200 mutated (TprC16M3), a third where the major sites and the minor site T2102 were mutated (TprC12M3), and a fourth where all four phosphorylation sites were mutated (TprC-M4). The phosphopeptide maps of in vitro-phosphorylated TprC and Tpr combination mutants (Fig. 4B, lower panel) demonstrated the absence of phosphorylation on major and minor peptides. These maps also showed increased phosphorylation of other sites, which likely represents hyperphosphorylation of the remaining minor sites. Most importantly, the TprC-M4 peptide map demonstrated the complete disappearance of ERK2-mediated phosphorylation. Incorporation of ^{32}P into TprC, TprC-M4, and the control was quantified by Cerenkov counting (Fig. 4C) and plotted as the percentage counts calculated with respect to counts in TprC (fixed at 100%). Mutating all four sites decreased the phosphorylation of Tpr by ~90% (Fig. 4C). Based on these results, we conclude that Thr2123 and Ser2141 are the major ERK2-mediated phosphorylation sites and Thr2102 and Thr2200 are minor ERK2-mediated phosphorylation sites on Tpr in vitro.

ERK2 phosphorylates Tpr at the same sites in vivo and in vitro. To determine if the same Tpr sites are utilized by ERK2 in vivo and in vitro, cells transfected with FLAG-TprFL and FLAG-TprC were metabolically labeled with ^{32}Pi with or without EGF stimulation. We observed a reproducible ~1.3-fold increase in levels of phosphorylation upon EGF stimulation (data not shown). Blocking the ERK activation with MEK inhibitor UO126 resulted in an ~50% decrease in phosphorylation levels of TprFL and TprC compared to levels in EGF-stimulated samples (data not shown). Tryptic peptide maps obtained for TprC with and without EGF stimulation were similar except for a slight increase in the intensity of spots (Fig. 5A). This is in keeping with earlier results where some interaction of Tpr with ERK2 was detected even in non-EGF-

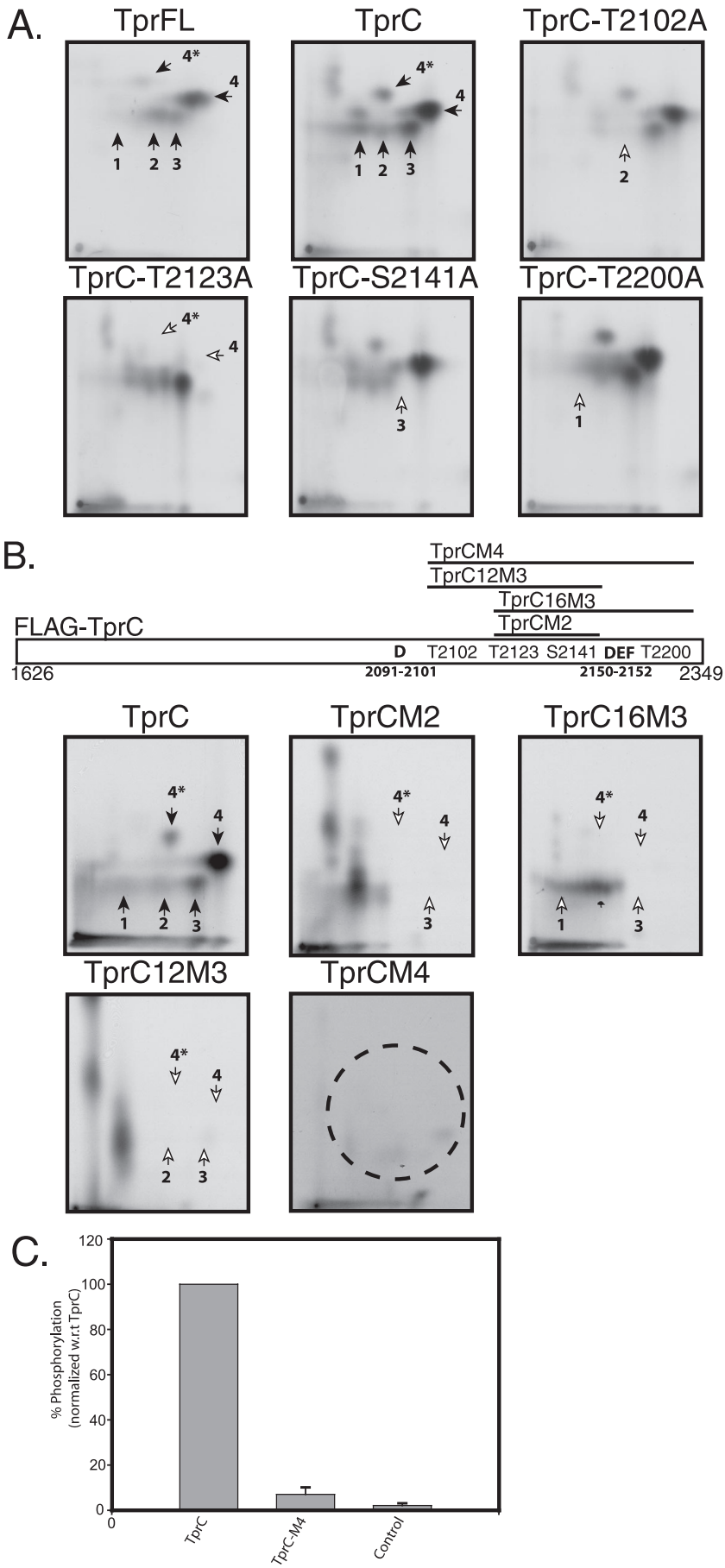

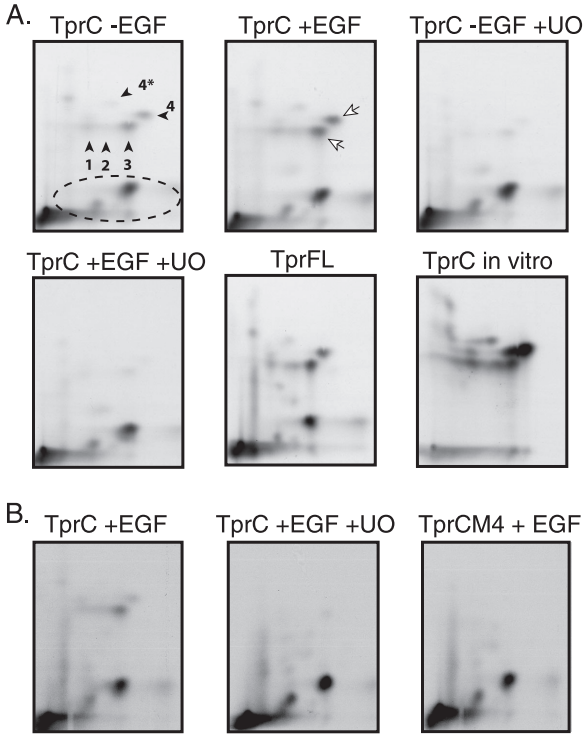

FIG. 5. ERK2 phosphorylates Tpr at the same sites in vivo and in vitro. (A) COS-1 cells were transfected with FLAG-TprFL or FLAG-TprC vectors. Transfected cells were labeled metabolically for 3 h. For the EGF-stimulated samples, EGF (20 ng/ml) was added after 3 h to the labeling cells for 10 min. For samples with MEK inhibitor UO126, 20 μM of inhibitor was present during the 3-h labeling and EGF stimulation. FLAG-tagged TprFL and TprC were immunoprecipitated, resolved, transferred, and autoradiographed. In vivo-labeled TprFL and TprC were digested with trypsin, and the resulting phosphopeptides were mapped by two-dimensional TLC. In vitro-labeled TprC from the earlier experiment was resolved on TLC plates along with in vivo-labeled TprC and TprFL. Peptide spots that show slight increases in intensity following EGF stimulation are indicated by white arrows (panel 2). Spots that did not disappear with UO126 pretreatment are marked in the first panel by a dotted line. (B) FLAG-TprC- and FLAG-TprC-M4-transfected cells were metabolically labeled as described above with EGF stimulation. Tryptic digested peptides were resolved by two-dimensional TLC (4).

stimulated cells (Fig. 1 and 2), which is possibly due to the fact that serum starvation does not completely eliminate activated ERK from these cells. Pretreatment of cells with the MEK inhibitor UO126 abolished the emergence of the tryptic peptides numbered 1, 2, 3, 4, and 4*, demonstrating that phosphorylation on these peptides depends on activation of ERK. In addition, we also detected tryptic peptides that are not affected by EGF treatment or UO126 pretreatment (Fig. 5A). These most likely arise from phosphorylation by other cellular kinases. In vivo-labeled full-length Tpr (TprFL) and C-terminal Tpr fragment (TprC) peptide maps were almost identical, suggesting that all the ERK-dependent and -independent phosphorylations are in the C-terminal 800 amino acids of Tpr. Comparison of the tryptic peptide maps of in vivo- and in vitro-labeled Tpr (Fig. 5A) showed that peptides which disappear upon UO126 pretreatment migrate at the same position on the thin-layer chromatography (TLC) plates as the in vitro phosphorylated peptides, indicating that these peptides were likely phosphorylated by ERK2.

To conclusively prove that the UO126-sensitive tryptic peptides detected with in vivo labeling were actually the same peptides detected in an in vitro kinase reaction, we performed another in vivo labeling experiment with TprC and TprC-M4. We observed that total phosphorylation levels of TprC in UO126-treated cells, as well as of TprC-M4, were 50% lower than that of TprC from EGF-stimulated cells (data not shown). Peptide maps obtained for TprC from UO126-treated cells and for TprC-M4 were identical (Fig. 5B). This implies that the effect of UO126 pretreatment of cells is similar to the effect of mutating all the phosphorylation sites of Tpr (TprC-M4 mutant). These results provide compelling evidence that ERK2 phosphorylates TprFL and TprC in vivo on the same target sites that were mapped in vitro.

Tpr-ERK2 interaction requires ERK2 phosphorylation and dimerization but not the D domain. Because Tpr bound only to activated ERKs, we examined the molecular mechanism by which ERK activation enabled Tpr binding. In the inactive state, ERKs are anchored to MEKs in the cytoplasm. Following cell stimulation and activation, ERKs are reported to dimerize and migrate into the nucleus (22). To decipher the structural and functional requirements of ERK in mediating the Tpr-ERK interaction, we utilized well-characterized ERK2 mutants. Endogenous Tpr coimmunoprecipitated efficiently with wild-type ERK2 following activation but not with the phosphorylation site mutant ERK2-TAYF (Fig. 6A). Since phosphorylation of ERK2 is a prerequisite for dimerization, we asked whether ERK2 dimerization is essential for Tpr binding. While Tpr coimmunoprecipitated with activated wild-type ERK2, no interaction was detectable with the ERK2 dimer-

FIG. 4. Tpr is phosphorylated by ERK2 at four different sites. (A) COS-1 cells were transfected with FLAG-TprFL, FLAG-TprC, and FLAG-TprC mutants (as specified above the maps). The immunoprecipitated FLAG-tagged Tpr proteins were mixed with immunoprecipitated FLAG-ERK2, and kinase reactions were carried out with [γ-^{32}P]ATP. In vitro-phosphorylated FLAG-tagged TprFL, TprC, and TprC mutants were digested with trypsin, and the resulting phosphopeptides were mapped by two-dimensional separation on TLC. Spots in similar positions in TprFL and TprC maps are indicated by numbered black arrows. Spots missing due to mutations in the TprC phosphorylation sites are indicated by numbered white arrows. (B) The upper panel depicts the nomenclature of the combination target site mutants of TprC. The putative D domain (^{2091}**RR**QSVGRG**L**Q**L**^{2101}) and DEF motif (^{2150}**F**R**F**^{2152}) are also indicated (residues that match the consensus for each motif are indicated by bold). In vitro-phosphorylated proteins were digested with trypsin, and the resulting phosphopeptides were mapped by TLC (4). Major (spots 3, 4, and 4*) and minor (spots 1 and 2) spots in TprC are indicated by numbered black arrows. Missing spots in TprCM2, TprC16M3, and TprC12M3 are indicated by numbered white arrows. In TprC-M4, the location of the missing spots is circled by a dotted line. (C) Incorporation of ^{32}P in in vitro-phosphorylated TprC, TprC-M4, and the vector control samples was quantified by Cerenkov counting in three independent experiments. Counts in TprC were normalized to 100% in each experiment, and the percent counts in other samples were calculated with respect to TprC. The results were plotted with percent counts with respect to TprC on the *y* axis and the samples on the *x* axis.

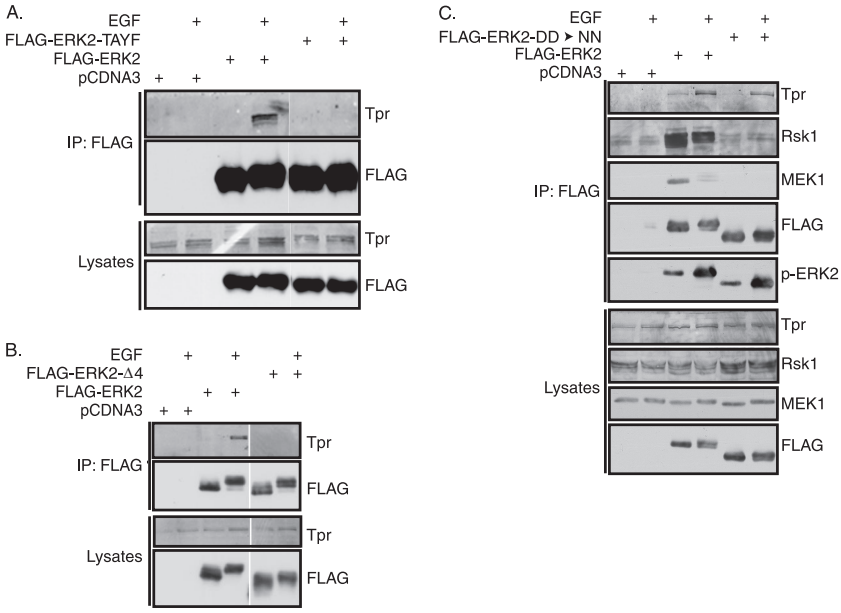

FIG. 6. Tpr-ERK2 interaction requires ERK2 phosphorylation and dimerization, but not the D domain. (A) Cells transfected with pcDNA3, FLAG-ERK2, and the FLAG-ERK2-TAYF mutant were serum starved and stimulated with EGF. Proteins immunoprecipitated (IP) with FLAG-M2 agarose beads from lysed cells were immunoblotted and probed with anti-FLAG and anti-Tpr antibodies. (B) Cells transfected with pcDNA3, FLAG-ERK2, and the FLAG-ERK2-Δ4 dimerization mutant were serum starved and stimulated with EGF. Proteins immunoprecipitated with FLAG-M2 agarose beads were immunoblotted and probed with anti-FLAG and anti-Tpr antibodies. (C) COS-1 cells transfected with pcDNA3, FLAG-ERK2, and FLAG-ERK2-DD→NN were serum starved, followed by stimulation with EGF as usual. Proteins immunoprecipitated from lysed cells with α-FLAG-M2 agarose beads were immunoblotted, and lysates and immunoprecipitates were probed with anti-FLAG and anti-MEK1 mouse monoclonal (Transduction Laboratories), anti-Rsk1 goat polyclonal (Santa Cruz Biotechnology Inc.), and anti-Tpr antibodies.

ization mutant FLAG-ERK2-Δ4 (Fig. 6B). These results demonstrate that Tpr-ERK2 interaction requires both phosphorylation of ERK2 (on TEY residues) and its dimerization.

The Tpr sequences required for ERK interaction were investigated next. The known ERK2-interacting proteins associate with ERK2 through either a KIM (D domain) or a docking domain (DEF motif) or both. Putative D domain (^{2091}RRX$_6$LXL^{2101}) and DEF motif (^{2150}FXF^{2152}) sequences are found in the C-terminal region. Mutating D316 and D319 in ERK2 is reported to abolish association with proteins containing a D domain (42). However, these mutations did not affect the interaction with Tpr; but they did abolish interaction with two other known binding proteins, MEK1 and Rsk1, as reported in the literature (42) (Fig. 6C).

ERK2 interacts with Tpr through DEF and phosphorylation sites. Next, we investigated whether ERK associates with Tpr through a DEF motif. It has been shown that the phosphorylation of T183 and Y185 residues on ERK2 causes a conformational change that results in the interaction of pY185, M197, L198, Y231, and L232 residues on the ERK2 surface, with two phenylalanine residues in the DEF motif-containing peptides (24). We found that ERK2 mutated at L232 did not associate with TprC (Fig. 7A), and conversely, TprC with a mutated DEF domain (FXF→AXA) showed decreased association with ERK2 (Fig. 7C; ~50%). These data strongly suggest that the interaction of ERK2 with Tpr occurs via the DEF domain on Tpr. However, to our surprise, we also detected decreased interaction of TprC-M4 with ERK2 compared to that of the wild type (Fig. 7B and C; ~60%). These results were intriguing, as they suggested that ERK phosphorylation sites in Tpr might be involved in the ERK-Tpr binding interaction. To further investigate this observation, we generated two more Tpr mutants: FLAG-TprC-FXF→AXA,M4, a combination mutant of phosphorylation sites and DEF mutations, and FLAG-TprC-Δ60, a deletion of 60 amino acids encompassing DEF and two major and one minor phosphorylation sites. Significantly, when we utilized a combination mutant of docking domain and phosphorylation sites (TprC-FXF→AXA,M4) or a TprC-Δ60 mutant, we could barely detect any interaction between Tpr and ERK2 (Fig. 7B and C; ~5%). These results show that the interaction between ERK2 and Tpr is through the mutually reinforcing combination of the DEF motif and the Tpr phosphorylation sites.

ERK2 interaction with Tpr is enhanced by phosphorylation. Our results strongly suggested that the target phosphorylation sites and DEF domain in Tpr cooperate in enhancing its interaction with ERK2. The interaction of target phosphorylation sites on Tpr with ERK2 could be mediated through the hydroxyl groups on serine/threonine residues, or alternatively, the interaction could be mediated through the phosphorylated serine/threonine residues. In order to distinguish between these possibilities, we looked at the interaction of HA-ERK2 and the kinase-inactive HA-ERK2-K52R (33) with FLAG-TprC and FLAG-TprC-FXF→AXA (Fig. 8). Though ERK2-K52R has very low kinase activity, it is efficiently phosphorylated on TEY residues (20), which is necessary for ERK2-Tpr interaction. If the interaction is through the DEF and the hydroxyl groups of target serine/threonine residues, there should not be any difference in the binding efficiencies of TprC with activated ERK2 and ERK2-K52R. Furthermore, this

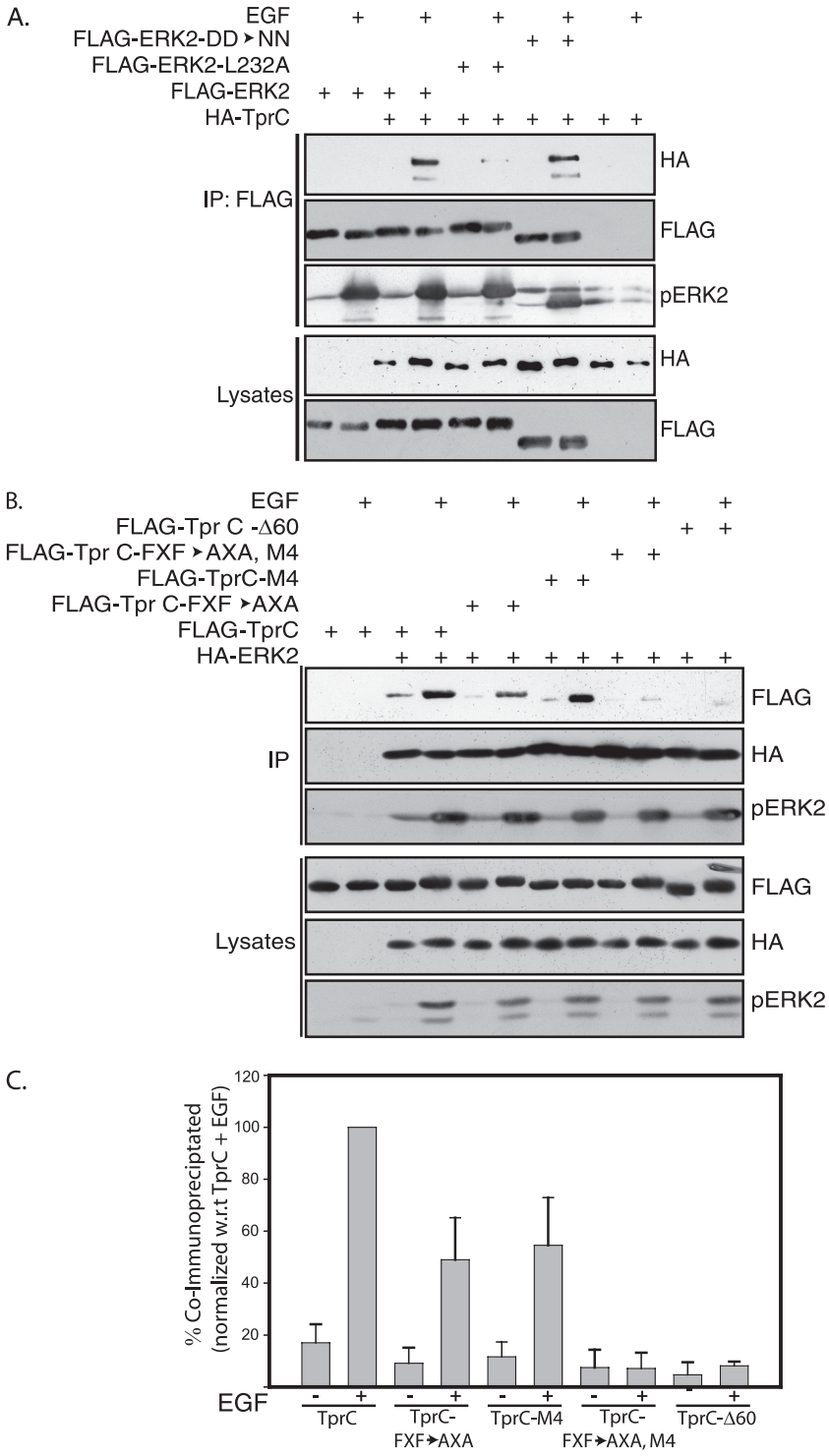

FIG. 7. ERK2 interacts with Tpr through DEF and phosphorylation sites. (A) Cells were cotransfected with FLAG-ERK2 or FLAG-ERK2-DD→NN or FLAG-ERK2 L232A or pcDNA3 and HA-TprC. Following serum starvation and EGF stimulation, proteins were immunoprecipitated (IP) with anti-FLAG antibodies. Lysates and immunoprecipitated proteins were probed with anti-FLAG and anti-HA antibodies. Immunoprecipitates were also probed with α-phospho-ERK antibodies. (B) Cells were transfected with FLAG-TprC or HA-ERK2 or double transfected with FLAG-TprC or FLAG-TprC-FXF→AXA, FLAG-TprC-M4, or FLAG-TprC-FXF→AXA,M4 or FLAG-TprC-Δ60 and HA-ERK2. Following serum starvation and EGF stimulation, proteins were immunoprecipitated with anti-HA antibodies. Lysates and immunoprecipitated proteins were probed with anti-FLAG, anti-HA, and anti-phospho-ERK antibodies. (C) Appropriate enhanced chemiluminescence exposures that are within the linear range of the X-ray film were used for quantitating coimmunoprecipitated wild-type and Tpr mutants using Image J software (Wayne Rasband, National Institutes of Health). Presence (+) or absence (−) of EGF and the sample names are indicated. Values obtained for the TprC+EGF sample were set at 100%. Percent binding values for the remaining samples were calculated with respect to TprC+EGF in each experiment. Percent binding values from three independent experiments were used for calculating standard deviations.

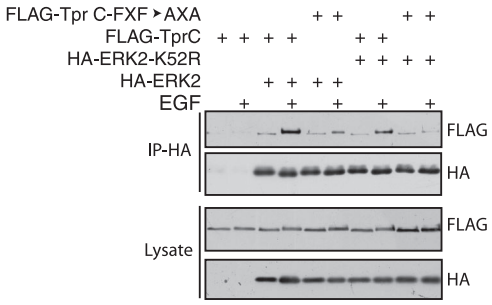

FIG. 8. Tpr phosphorylation enhances ERK2-Tpr binding. (A) Cells were cotransfected with pcDNA3 or HA-ERK2 or HA-ERK2-K52R and FLAG-TprC or FLAG-TprC-FXF→AXA. Following serum starvation and EGF stimulation, proteins were immunoprecipitated (IP) with anti-HA beads (Sigma). Lysates and immunoprecipitated proteins were probed with anti-FLAG and anti-HA antibodies.

model also predicts that ERK2 and ERK2-K52R will associate equally well with TprC-FXF→AXA, where the DEF motif is mutated. However, if the phosphorylation of target serine/threonine residues is required for the interaction, one would expect decreased interactions of TprC with ERK2-K52R compared with those for ERK2. Since ERK2-K52R does not possess kinase activity, its interaction with TprC should be similar to that of the ERK2 interaction with TprC-M4. Results obtained in Fig. 8 agree well with this prediction. Likewise, ERK2-K52R interaction with TprC-FXF→AXA should be similar to that of ERK2 with TprC-FXF→AXA,M4. It is evident from the data (Fig. 8) that the TprC-FXF→AXA interaction with ERK2-K52R is almost negligible. These results suggest that the interaction of ERK2 with Tpr is through DEF and that the phosphorylated serine/threonine residues and the phosphorylation of Tpr by ERK2 increase their interaction.

ERK2 phosphorylates proteins that interact with Tpr. The fact that the ERK-Tpr interaction is stabilized by phosphorylation of serine/threonine residues suggests that Tpr provides a stable docking site for active ERK2. This would allow the active ERK2 to be tethered to the nuclear pore and phosphorylate other proteins in *trans*, including proteins that are transiting the nuclear pore. To test this hypothesis, we looked for ERK substrates in immunoprecipitates of Tpr. COS-1 cells were cotransfected with HA-ERK2 or HA-ERK2-QG and FLAG-TprFL or the TprFL-FXF→AXA,M4 mutant. As anticipated, ERK2 or ERK2-QG coimmunoprecipitated with the wild-type TprFL but not with the mutant TprFL-FXF→AXA,M4 (Fig. 9A), which is in agreement with our results in Fig. 7B. To detect substrates of Tpr-associated ERK2, we performed in vitro kinase reactions with these immunoprecipitates, using the ATP analog [γ-^{32}P]cpATP. Since [γ-^{32}P]cpATP is selectively utilized by ERK2-QG, the direct ERK2 substrates will become radiolabeled in immunoprecipitates that contain ERK2-QG and wild-type Tpr but not in those that contain wild-type ERK2 (which cannot utilize the analog) nor in immunoprecipitates of Tpr FXF→AXA,M4. As Tpr is a substrate for ERK2, we detected significant phosphorylation of Tpr by ERK2-QG (Fig. 9B). In addition, we detected another radiolabeled band at ~70 kDa (Fig. 9B), indicating phosphorylation of an additional Tpr-interacting protein by the Tpr-bound active ERK2. Moreover, when the resolution of the gel system was increased by using two-dimensional gels, we detected more spots indicative of direct phosphorylations by Tpr-tethered ERK2 (Fig. 9C, middle panel). These data suggest that ER2K phosphorylated the proteins that interact with Tpr and that the ERK2-Tpr association is necessary for this process.

Tpr regulates YFP-ERK2 recruitment into the nucleus in response to EGF treatment. In addition to Tpr, previous reports have shown that ERK associates with other components of the nuclear pore complex, nucleoporins Nup153 and Nup214. These findings suggested that ERK binding to nuclear pore complex proteins could facilitate the translocation of activated ERK2 from the cytoplasm to the nucleus (26, 46). We thus tested whether Tpr plays any role in nuclear transport of ERKs by depleting the cells of Tpr using double-stranded siRNA. We could effectively deplete the cells of Tpr protein (Fig. 10A), and they remained depleted until 96 h (data not shown). Tpr siRNA-treated HEK293T cells previously transfected with CFP-MEK1 and YFP-ERK2 were serum starved, followed by EGF stimulation. Localization of YFP-ERK2 in the nucleus before and after EGF stimulation was monitored by fluorescence microscopy. As shown in Fig. 10B, Tpr attenuation resulted in decreased recruitment of YFP-ERK2 into the nucleus. In addition, we observed that overexpression of full-length Tpr led to decreased translocation of YFP-ERK2 to the nucleus in response to EGF stimulation (Fig. 10C). This could be due to sequestration of YFP-ERK2 by overexpressed Tpr or due to sequestration of other proteins that may be required for ERK2 translocation, thus decreasing the nuclear levels of ERK2. Based on these data, we deduce that either attenuation or overexpression of Tpr blocks YFP-ERK2 localization to the nucleus. Collectively, our data demonstrate that Tpr plays a role in modulating the translocation of activated ERK2 from the cytoplasm to the nucleus and that this regulation is dependent on the amount of Tpr present in the cells.

DISCUSSION

In this study, we present evidence that Tpr is a bona fide ERK2 substrate in vivo. We have shown that Tpr is a direct substrate for ERK2 in cell lysates and in vitro, that the sites of in vitro phosphorylation by MAPK are identical to a subset of in vivo phosphorylation sites, and that these specific phosphorylations disappeared after blockade of the MAPK ERK2 pathway. We also show that ERK2 binds to Tpr and have identified both the docking domains on Tpr and the complementary domain on ERK2. We show that phosphorylation of Tpr by ERK stabilizes the interaction between these proteins and that this interaction positions ERK2 for phosphorylation of other substrates. Finally, we provide evidence that the ERK-Tpr interaction regulates nuclear translocation of ERK2. Collectively, the findings develop a picture of activated ERK2 interacting with Tpr to enhance its nuclear uptake and to phosphorylate other proteins that either are transiting through the pore or may be involved in nuclear pore function.

Tpr-ERK2 interaction motifs. The D and DEF domains are structural elements important for efficient interaction of diverse sets of proteins with MAPKs (41, 44). The D domain associates promiscuously with MAPK family members, including ERK, JNK, and p38 (42, 43). On the other hand, the FXF

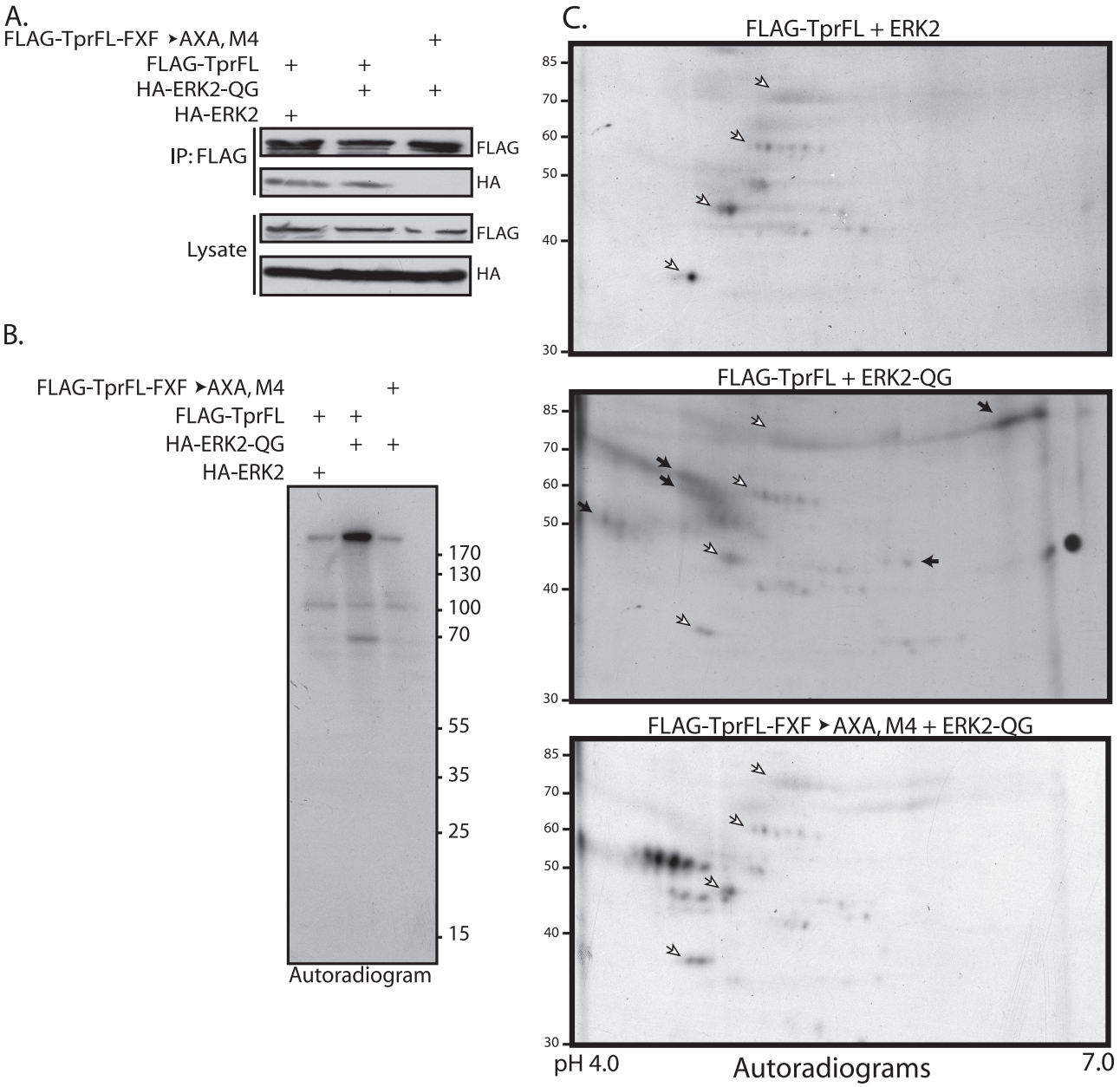

FIG. 9. ERK2 phosphorylates proteins that interact with Tpr. (A) COS-1 cells were cotransfected with FLAG-TprFL or FLAG-TprFL-FXF→AXA,M4 and HA-ERK2 or HA-ERK2-QG. Cells were serum starved and stimulated with 20 ng/ml EGF, and the proteins were immunoprecipitated (IP) with FLAG-M2 agarose beads. In vitro kinase reactions were carried out with 1/10 of the immunoprecipitated proteins, and part of the lysate was resolved by SDS-PAGE, transferred onto a nitrocellulose membrane, and probed with anti-FLAG and anti-HA antibodies. (B) Kinase reactions were carried out with the remaining 9/10 of immunoprecipitated proteins by using ~20 μCi [γ-^{32}P]cpATP (analog ATP) as the substrate for 15 min at 30°C. One-fifth of the volume of these reaction mixtures was resolved by SDS-PAGE, transferred onto a nitrocellulose membrane, and autoradiographed. (C) The remaining part of the kinase reaction mixtures was resolved on pH 4 to 7 two-dimensional gels as described in our previous report (10). Background spots indicated by white arrows were used for aligning the autoradiograms. Additional spots that are specifically detected in TprFL+ERK2-QG reactions (middle panel) are indicated by black arrows.

motif of the DEF domain specifically associates with ERK and does not mediate the interaction with JNK and p38, probably due to steric constraints in JNK and p38 (21, 24, 47). Our observation that Tpr interacts with ERK primarily through the FXF motif of the DEF domain suggested that Tpr would specifically associate with ERKs. Indeed, Tpr associated specifically with ERK2 and ERK1 but not with the close family member JNK1 or p38α or the ERK upstream activator MEK1 (Fig. 2). Structural and biochemical studies showed that ERK preferentially phosphorylates residues that are located close to the N terminus of the DEF domain (11, 21, 24). Consistent with this, we found that the major Tpr phosphorylation sites are located N terminally of the DEF domain. Moreover, because kinase-defective ERK2-K52R is less effective at binding

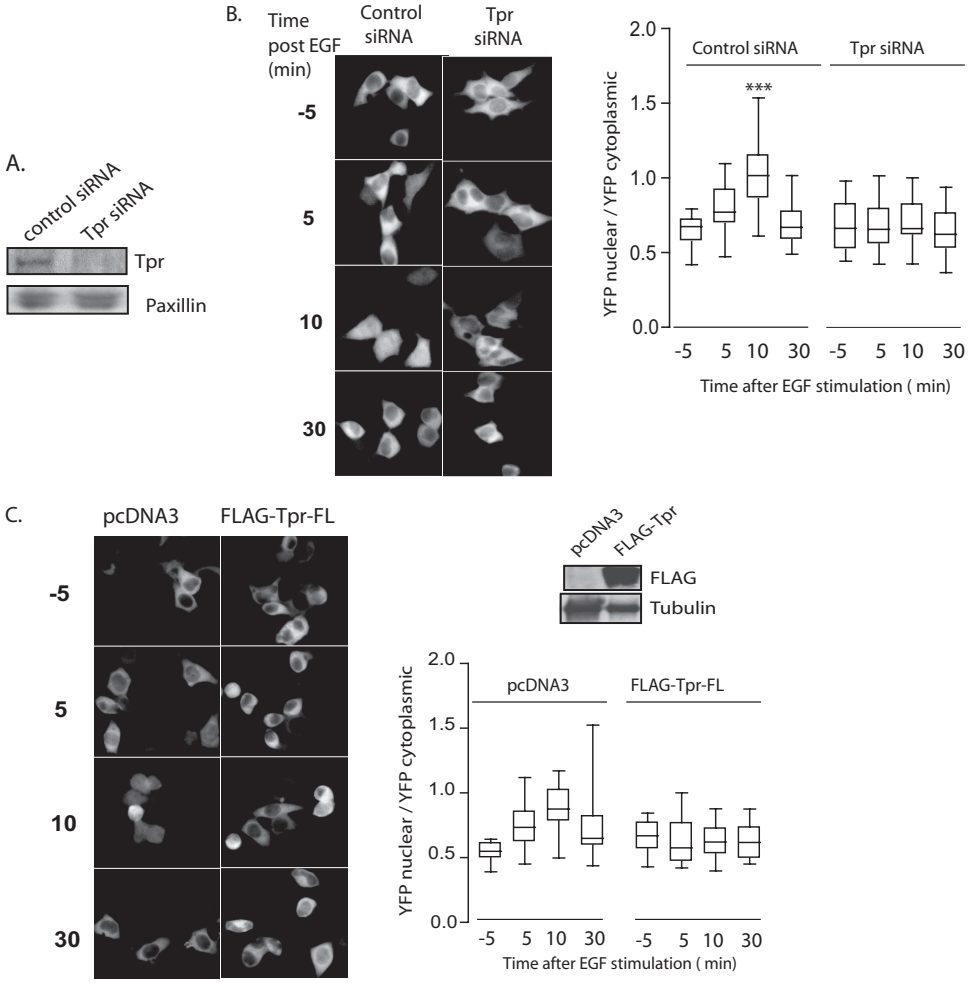

FIG. 10. Tpr regulates YFP-ERK recruitment into the nucleus in response to EGF stimulation. Control- or Tpr siRNA-treated HEK293T cells expressing CFP-MEK and YFP-ERK were plated on glass dishes coated with extracellular matrix components (10 μg/ml fibronectin and 5 μg/ml collagen type IV). The next day, cells were serum deprived for 3 h and stimulated with EGF (10 ng/ml). (A) Western blot analysis of Tpr expression in control and Tpr siRNA-treated cells. Lysates from control and Tpr knockdown cells were probed with antiTpr and antipaxillin antibody as described in Materials and Methods. (B) Images of and quantification of YFP-ERK nuclear localization in control and Tpr siRNA-treated HEK293T cells prior to and after EGF stimulation. (C) Images show the quantification of YFP-ERK in pcDNA3- or Flag-Tpr-expressing cells prior to and after EGF stimulation and Western blot analysis of Flag-Tpr expression in pcDNA3- and Flag-Tpr-expressing cells. In panels B and C, approximately 50 to 70 cells per each experimental condition were used to quantify YFP-ERK translocation to the nucleus. Each experiment was repeated twice.

than the wild-type ERK2, it is likely that the phosphorylation of Tpr occurs in *cis* by the kinase molecule that is bound to the Tpr. Together, these data indicate that the DEF domain of Tpr has a dual function, as it specifically selects ERK and directs ERK activity toward specific phosphorylation sites on Tpr.

Tpr functions. Nucleoporin Tpr was reported to play a role in the export of leucine-rich nuclear export signal-containing proteins (14). In order to investigate the role of ERK-mediated phosphorylation of Tpr on the import/export of proteins, we utilized a hormone-inducible, GFP-labeled chimeric Rev protein (Rev/GR/GFP) construct developed by Love et al. (25). We did not detect any significant difference in the import or export of the Rev/GR/GFP protein between wild-type and Tpr-depleted COS-1 cells (data not shown). In agreement with these findings, Shibata et al. (39) reported that depleting nuclei of Tpr by microinjection with Tpr antibody did not alter either protein import or export. Contrasting results obtained by Frosst et al. (14) and our group could be due to differences in the types of cell lines and the fact that they used antibody injection whereas we used siRNA as a mechanism for depleting Tpr (data not shown).

The yeast homolog Mlp1 was shown to be involved in the nuclear retention of unspliced mRNAs (16). These data imply a possible role for Tpr in the export of unspliced mRNA. Knockdown of Tpr with siRNA resulted in increased export of unspliced RNA as measured by production of the HIV *gag* gene product p24 in the supernatant (J. Coyle, D. Rekosh, and M.-L. Hammarskjold, personal communication). We hypothesized that ERK binding and phosphorylation could alter this measurable Tpr function, but experiments carried out by us in

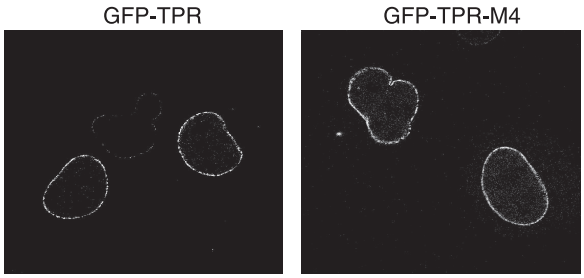

FIG. 11. Localization of GFP-Tpr and GFP-Tpr-M4. Images show the confocal microscopy of COS-1 cells transfected with GFP-Tpr or GFP-Tpr-M4 (as described in Materials and Methods).

collaboration with Coyle et al. did not provide evidence that ERK2-mediated phosphorylation of Tpr plays a role in the export of unspliced mRNAs (data not shown).

Role of Tpr-ERK2 interaction. ERK binding could play a role in the localization of Tpr to the nuclear pore, as has been observed in the case of the cyclin-dependent kinase inhibitor p27kip1 (13) and NFATc (*n*uclear *f*actor of *a*ctivated *T c*ells) (31). However, expression of Tpr-M4, which associates poorly with ERK2 and cannot be phosphorylated by it, localized normally in the nuclear membrane as judged by immunofluorescence (Fig. 11). Previous studies implicated ERK2 interaction with nucleoporins Nup153 and -214 in the translocation of both unphosphorylated and phosphorylated ERK2 (26, 46). Mutants of ERK2 defective in interaction with the FXF motif of DEF domain-containing proteins show decreased rates of nuclear import. This was proposed to be due to the decreased interaction of mutant ERK2 protein with nucleoporin Nup153 (48). However, translocation of wild-type and mutant GFP-ERK2 in Nup153-depleted cells was not measured. Since the interaction of ERK2 with Tpr is through the DEF domain, we speculated that Tpr might play a role in modulating the translocation of ERK2 into the nucleus. In agreement with these predictions, depletion or overexpression of Tpr resulted in decreased localization of ERK2 upon EGF stimulation (Fig. 10). The fact that either depletion or overexpression of Tpr interfered with ERK translocation is consistent with our proposal that Tpr functions both as an ERK substrate and as an ERK scaffold: it is characteristic of scaffold proteins that appropriate stoichiometry of all the components is necessary for accurate function (35).

Our finding that the DEF domain and phosphorylation of Tpr mutually enhance the Tpr-ERK interaction was surprising, and it raises questions as to the role such a positive feedback might play in cell function. Some of the best-characterized ERK substrates decrease their association with ERK after they are phosphorylated (e.g., p90RSK; see Fig. 6C and reference 34). This allows the substrate to move to its site of action and for the activated ERK to service several substrate proteins, thus amplifying the signaling cascade. However, stable association between substrate and kinase suggests that Tpr serves both as a substrate and as a scaffold. This would allow the active ERK2 to be tethered to the nuclear pore and to phosphorylate various proteins that are transiting the nuclear pore. A similar concept has recently been proposed by Pokholok et al. (30), who reported that yeast MAPKs stably associate with appropriate specific gene promoters and phosphorylate multiple components of the transcription machinery. An analogous premise was previously suggested for ERK recruitment by the Fos transcription factor through its DEF domain, which was required for Fos phosphorylation. This interaction through the DEF domain was proposed to have wider functional implications that include transphosphorylation of proteins associated with Fos in the AP1 transcription complex (27). Consistent with these concepts, we found that the ERK2-QG "pocket" mutant specifically phosphorylated proteins that interact with Tpr (Fig. 9). The low levels of these proteins precluded their identification in these experiments, but future studies that identify the substrates of Tpr-bound ERK should provide insight into the ways that the substrate and scaffold functions of Tpr interact in nuclear transport.

ACKNOWLEDGMENTS

This work is supported by intramural and extramural funding provided by the Department of Biotechnology, India, to V.K.N., grants R01 CA105402, P01 CA040042, and P01 CA076465 to M.J.W. from the National Institute of Health and the Academy of Sciences of the Czech Republic Institutional Research Concept AV0Z50200510, and grant IAA500200716 to T.V.

D.T. is a Senior Research Fellow of the Council of Scientific and Industrial Research.

We thank members of the Parsons-Weber-Parsons group for helpful discussions; Scott Eblen for the FLAG-ERK2-TAYF and FLAG-ERK2-K52R constructs; Larry Gerace, Melanie Cobb, Dennis J. Templeton, and Roger Davis for materials used in this study; John Coyle, Marie-Louise Hammarskjold, and David Rekosh for assistance in testing the effects of Tpr phosphorylation on nuclear transport; and Swati Saha for critical reading of the manuscript.

REFERENCES

1. **Adachi, M., M. Fukuda, and E. Nishida.** 1999. Two co-existing mechanisms for nuclear import of MAP kinase: passive diffusion of a monomer and active transport of a dimer. EMBO J. **18:**5347–5358.
2. **Bangs, P., B. Burke, C. Powers, R. Craig, A. Purohit, and S. Doxsey.** 1998. Functional analysis of Tpr: identification of nuclear pore complex association and nuclear localization domains and a role in mRNA export. J. Cell Biol. **143:**1801–1812.
3. **Biondi, R. M., and A. R. Nebreda.** 2003. Signalling specificity of Ser/Thr protein kinases through docking-site-mediated interactions. Biochem. J. **372:** 1–13.
4. **Boyle, W. J., P. van der Geer, and T. Hunter.** 1991. Phosphopeptide mapping and phosphoamino acid analysis by two-dimensional separation on thin-layer cellulose plates. Methods Enzymol. **201:**110–149.
5. **Burack, W. R., and A. S. Shaw.** 2005. Live cell imaging of ERK and MEK: simple binding equilibrium explains the regulated nucleocytoplasmic distribution of ERK. J. Biol. Chem. **280:**3832–3837.
6. **Canagarajah, B. J., A. Khokhlatchev, M. H. Cobb, and E. J. Goldsmith.** 1997. Activation mechanism of the MAP kinase ERK2 by dual phosphorylation. Cell **90:**859–869.
7. **Chen, R. H., C. Abate, and J. Blenis.** 1993. Phosphorylation of the c-Fos transrepression domain by mitogen-activated protein kinase and 90-kDa ribosomal S6 kinase. Proc. Natl. Acad. Sci. USA **90:**10952–10956.
8. **Cornett, J., F. Cao, C. E. Wang, C. A. Ross, G. P. Bates, S. H. Li, and X. J. Li.** 2005. Polyglutamine expansion of huntingtin impairs its nuclear export. Nat. Genet. **37:**198–204.
9. **Derijard, B., M. Hibi, I. H. Wu, T. Barrett, B. Su, T. Deng, M. Karin, and R. J. Davis.** 1994. JNK1: a protein kinase stimulated by UV light and Ha-Ras that binds and phosphorylates the c-Jun activation domain. Cell **76:**1025–1037.
10. **Eblen, S. T., N. V. Kumar, K. Shah, M. J. Henderson, C. K. Watts, K. M. Shokat, and M. J. Weber.** 2003. Identification of novel ERK2 substrates through use of an engineered kinase and ATP analogs. J. Biol. Chem. **278:**14926–14935.
11. **Fantz, D. A., D. Jacobs, D. Glossip, and K. Kornfeld.** 2001. Docking sites on substrate proteins direct extracellular signal-regulated kinase to phosphorylate specific residues. J. Biol. Chem. **276:**27256–27265.
12. **Fincham, V. J., M. James, M. C. Frame, and S. J. Winder.** 2000. Active ERK/MAP kinase is targeted to newly forming cell-matrix adhesions by integrin engagement and v-Src. EMBO J. **19:**2911–2923.

13. **Foster, J. S., R. I. Fernando, N. Ishida, K. I. Nakayama, and J. Wimalasena.** 2003. Estrogens down-regulate p27Kip1 in breast cancer cells through Skp2 and through nuclear export mediated by the ERK pathway. J. Biol. Chem. **278:**41355–41366.
14. **Frosst, P., T. Guan, C. Subauste, K. Hahn, and L. Gerace.** 2002. Tpr is localized within the nuclear basket of the pore complex and has a role in nuclear protein export. J. Cell Biol. **156:**617–630.
15. **Galanis, A., S. H. Yang, and A. D. Sharrocks.** 2001. Selective targeting of MAPKs to the ETS domain transcription factor SAP-1. J. Biol. Chem. **276:**965–973.
16. **Galy, V., O. Gadal, M. Fromont-Racine, A. Romano, A. Jacquier, and U. Nehrbass.** 2004. Nuclear retention of unspliced mRNAs in yeast is mediated by perinuclear Mlp1. Cell **116:**63–73.
17. **Gonzalez, F. A., D. L. Raden, and R. J. Davis.** 1991. Identification of substrate recognition determinants for human ERK1 and ERK2 protein kinases. J. Biol. Chem. **266:**22159–22163.
18. **Gonzalez, F. A., A. Seth, D. L. Raden, D. S. Bowman, F. S. Fay, and R. J. Davis.** 1993. Serum-induced translocation of mitogen-activated protein kinase to the cell surface ruffling membrane and the nucleus. J. Cell Biol. **122:**1089–1101.
19. **Greco, A., M. A. Pierotti, I. Bongarzone, S. Pagliardini, C. Lanzi, and P. G. Della.** 1992. TRK-T1 is a novel oncogene formed by the fusion of TPR and TRK genes in human papillary thyroid carcinomas. Oncogene **7:**237–242.
20. **Her, J. H., S. Lakhani, K. Zu, J. Vila, P. Dent., T. W. Sturgill, and M. J. Weber.** 1993. Dual phosphorylation and autophosphorylation in mitogen-activated protein (MAP) kinase activation. Biochem. J. **296:**25–31.
21. **Jacobs, D., D. Glossip, H. Xing, A. J. Muslin, and K. Kornfeld.** 1999. Multiple docking sites on substrate proteins form a modular system that mediates recognition by ERK MAP kinase. Genes Dev. **13:**163–175.
22. **Khokhlatchev, A. V., B. Canagarajah, J. Wilsbacher, M. Robinson, M. Atkinson, E. Goldsmith, and M. H. Cobb.** 1998. Phosphorylation of the MAP kinase ERK2 promotes its homodimerization and nuclear translocation. Cell **93:**605–615.
23. **King, H. W., P. R. Tempest, K. R. Merrifield, and A. J. Rance.** 1988. tpr homologues activate met and raf. Oncogene **2:**617–619.
24. **Lee, T., A. N. Hoofnagle, Y. Kabuyama, J. Stroud, X. Min, E. J. Goldsmith, L. Chen, K. A. Resing, and N. G. Ahn.** 2004. Docking motif interactions in MAP kinases revealed by hydrogen exchange mass spectrometry. Mol. Cell **14:**43–55.
25. **Love, D. C., T. D. Sweitzer, and J. A. Hanover.** 1998. Reconstitution of HIV-1 rev nuclear export: independent requirements for nuclear import and export. Proc. Natl. Acad. Sci. USA **95:**10608–10613.
26. **Matsubayashi, Y., M. Fukuda, and E. Nishida.** 2001. Evidence for existence of a nuclear pore complex-mediated, cytosol-independent pathway of nuclear translocation of ERK MAP kinase in permeabilized cells. J. Biol. Chem. **276:**41755–41760.
27. **Murphy, L. O., S. Smith, R. H. Chen, D. C. Fingar, and J. Blenis.** 2002. Molecular interpretation of ERK signal duration by immediate early gene products. Nat. Cell Biol. **4:**556–564.
28. **Nishida, E., and Y. Gotoh.** 1993. The MAP kinase cascade is essential for diverse signal transduction pathways. Trends Biochem. Sci. **18:**128–131.
29. **Park, M., M. Dean, C. S. Cooper, M. Schmidt, S. J. O'Brien, D. G. Blair, and G. F. Vande Woude.** 1986. Mechanism of met oncogene activation. Cell **45:**895–904.
30. **Pokholok, D. K., J. Zeitlinger, N. M. Hannett, D. B. Reynolds, and R. A. Young.** 2006. Activated signal transduction kinases frequently occupy target genes. Science **313:**533–536.
31. **Porter, C. M., M. A. Havens, and N. A. Clipstone.** 2000. Identification of amino acid residues and protein kinases involved in the regulation of NFATc subcellular localization. J. Biol. Chem. **275:**3543–3551.
32. **Robinson, M. J., M. Cheng, A. Khokhlatchev, D. Ebert, N. Ahn, K. L. Guan, B. Stein, E. Goldsmith, and M. H. Cobb.** 1996. Contributions of the mitogen-activated protein (MAP) kinase backbone and phosphorylation loop to MEK specificity. J. Biol. Chem. **271:**29734–29739.
33. **Rossomando, A. J., J. Wu, H. Michel, J. Shabanowitz, D. F. Hunt, M. J. Weber, and T. W. Sturgill.** 1992. Identification of Tyr-185 as the site of tyrosine autophosphorylation of recombinant mitogen-activated protein kinase p42mapk. Proc. Natl. Acad. Sci. USA **89:**5779–5783.
34. **Roux, P. P., S. A. Richards, and J. Blenis.** 2003. Phosphorylation of p90 ribosomal S6 kinase (RSK) regulates extracellular signal-regulated kinase docking and RSK activity. Mol. Cell. Biol. **23:**4796–4804.
35. **Schaeffer, H. J., A. D. Catling, S. T. Eblen, L. S. Collier, A. Krauss, and M. J. Weber.** 1998. MP1: a MEK binding partner that enhances enzymatic activation of the MAP kinase cascade. Science **281:**1668–1671.
36. **Seanor, K. L., J. V. Cross, S. M. Nguyen, M. Yan, and D. J. Templeton.** 2003. Reactive quinones differentially regulate SAPK/JNK and p38/mHOG stress kinases. Antioxid. Redox Signal. **5:**103–113.
37. **Shah, K., Y. Liu, C. Deirmengian, and K. M. Shokat.** 1997. Engineering unnatural nucleotide specificity for Rous sarcoma virus tyrosine kinase to uniquely label its direct substrates. Proc. Natl. Acad. Sci. USA **94:**3565–3570.
38. **Sharrocks, A. D., S. H. Yang, and A. Galanis.** 2000. Docking domains and substrate-specificity determination for MAP kinases. Trends Biochem. Sci. **25:**448–453.
39. **Shibata, S., Y. Matsuoka, and Y. Yoneda.** 2002. Nucleocytoplasmic transport of proteins and poly(A)+ RNA in reconstituted Tpr-less nuclei in living mammalian cells. Genes Cells **7:**421–434.
40. **Slack, J. K., A. D. Catling, S. T. Eblen, M. J. Weber, and J. T. Parsons.** 1999. c-Raf-mediated inhibition of epidermal growth factor-stimulated cell migration. J. Biol. Chem. **274:**27177–27184.
41. **Smith, J. A., C. E. Poteet-Smith, K. Malarkey, and T. W. Sturgill.** 1999. Identification of an extracellular signal-regulated kinase (ERK) docking site in ribosomal S6 kinase, a sequence critical for activation by ERK in vivo. J. Biol. Chem. **274:**2893–2898.
42. **Tanoue, T., M. Adachi, T. Moriguchi, and E. Nishida.** 2000. A conserved docking motif in MAP kinases common to substrates, activators and regulators. Nat. Cell Biol. **2:**110–116.
43. **Tanoue, T., and E. Nishida.** 2002. Docking interactions in the mitogen-activated protein kinase cascades. Pharmacol. Ther. **93:**193–202.
44. **Tanoue, T., and E. Nishida.** 2003. Molecular recognitions in the MAP kinase cascades. Cell. Signal. **15:**455–462.
45. **Whitehurst, A. W., F. L. Robinson, M. S. Moore, and M. H. Cobb.** 2004. The death effector domain protein PEA-15 prevents nuclear entry of ERK2 by inhibiting required interactions. J. Biol. Chem. **279:**12840–12847.
46. **Whitehurst, A. W., J. L. Wilsbacher, Y. You, K. Luby-Phelps, M. S. Moore, and M. H. Cobb.** 2002. ERK2 enters the nucleus by a carrier-independent mechanism. Proc. Natl. Acad. Sci. USA **99:**7496–7501.
47. **Yang, S. H., A. J. Whitmarsh, R. J. Davis, and A. D. Sharrocks.** 1998. Differential targeting of MAP kinases to the ETS-domain transcription factor Elk-1. EMBO J. **17:**1740–1749.
48. **Yazicioglu, M. N., D. L. Goad, A. Ranganathan, A. W. Whitehurst, E. J. Goldsmith, and M. H. Cobb.** 2007. Mutations in ERK2 binding sites affect nuclear entry. J. Biol. Chem. **282:**28759–28767.
49. **Yoon, S., and R. Seger.** 2006. The extracellular signal-regulated kinase: multiple substrates regulate diverse cellular functions. Growth Factors **24:** 21–44.
50. **Zhou, T., L. Sun, J. Humphreys, and E. J. Goldsmith.** 2006. Docking interactions induce exposure of activation loop in the MAP kinase ERK2. Structure **14:**1011–1019.